Resistance Dynamics in Chronic Lymphocytic Leukemia

Dua Fatima[*], Montana Ferita[†], Sarwesh Rauniyar[‡], and Ana Venerio[ξ]

[*]Lahore University of Management Sciences, PK
[†]University of Utah, UT
[‡]University of Washington, WA
[ξ]University of California San Diego, CA

July 29, 2021

Abstract

Chronic lymphocytic leukemia (CLL) is the most common form of adult leukemia. CLL develops through the unregulated proliferation of lymphocytes in the blood and bone marrow. Currently, CLL is treated with chemotherapy and targeted therapies. Over the course of treatment, patients may develop therapeutic resistance due to the accumulation of drug-resistant mutations. Previous research has studied the evolutionary dynamics of ibrutinib-resistant mutations in the absence and presence of ibrutinib, a targeted therapy. Expanding upon a previously proposed model, we analyze the mechanism behind resistance dynamics by incorporating density dependence. We use a discrete time birth-death process to model the growth of the CLL cells as well as the probability of developing resistance mutations. We explore how density dependence of tumor growth impacts the evolution of drug resistance in relation to the population size of resistance mutations and the relative frequencies of resistant sub-clones. We model the growth of the CLL cells logistically and compare our findings to models utilizing an exponential growth. Additionally, we analyze how variation in different parameters effect treatment duration such as the impact of susceptibility to treatment, time of treatment initiation, and mutation rate.

1 Introduction

Chronic Lymphocytic Leukemia (CLL) is the most common form of adult leukemia [6]. Currently, there is an estimated incidence of 4.7 new cases per 100,000 individuals. The median age at diagnosis is 70 years, with a male predominance (1.3:1) in all ethnic groups [6]. CLL develops due to unregulated proliferation of B cells in the bone marrow, lymph nodes, and the blood [6]. Currently, CLL is treated with chemotherapy and targeted therapies; however, there is no cure. In the absence of a cure, patients receive treatment for many years and over time can develop therapeutic resistance due to the accumulation of drug-resistant mutations.

CLL patients can be divided into two subgroups based on the presence or absence of mutations in the Immunoglobulin heavy chain variable region (IGHV) genes. The first subgroup is IGHV-mutated (IGHV-M) CLLs that are derived from antigen-experienced B cells that have transited through the germinal centre (GC) of secondary lymphoid organs. The second subgroup is the IGHV-ummutated (IGHV-UM) CLLs which are derived from pre-GC B cells. The field of CLL has been improved recently by the stereotypy of B cell receptor (BCR) and whole exome sequencing (WES) based discovery of specific mutations like NOTCH1, TP53, SF3B1, BIRC3, ATM, and RPS15 which has helped to develop systems for prognosis in CLL. The International Working Group of CLL (iwCLL) has established that the criteria for the diagnosis of CLL are monoclonal B lymphocytes $\geq$ 5000 lymphocytes/ml in the peripheral blood for a duration of at least three months and $\leq$ 55 prolymphocytes and flow cytometry showing co-expression of CD5 and B-cell surface antigens CD19, CD20, and CD23, low levels of sIg, CD20, CD79b and kappa or lambda light chain restriction [5].

The recent advances in anticancer agents have contributed significantly to the improvement of both the disease-free survival and quality of life in cancer patients. However, in many instances, a favorable initial response to treatment changes afterwards, thereby leading to cancer relapse and recurrence. In other cases, the initial optimism after a good treatment response is often followed by poor results and a devastating outcome, as tumors initially sensitive to therapy later become unresponsive due to the development of acquired drug resistance. This includes resistance to typical chemotherapeutic drugs such as purine analogs, alkylating agents, and corticosteroids. These drugs target rapidly proliferating cells but have many side effects include targeting other healthy, highly mitotic cell types [1].

There are two kinds of drug resistance when some of the cells that are not killed by chemotherapy mutate and become resistant to the drug: intrinsic and acquired drug resistance [1]. *Intrinsic Resistance* can be attributed to drug breakdown, altered expression and/or function of the drug

target, altered drug transport across the cellular membrane or reduced interaction efficiency between the drug and its molecular target. Additionally, cellular metabolic processes that inhibit chemotherapeutic agents, cell cycle regulators and DNA damage repair factors also enhance cross-drug resistance by inhibiting drug accumulation, reducing influx, increasing efflux through cell membrane transporters, or inactivating drugs [1]. *Acquired Drug Resistance* is influenced by genetic or environmental factors that facilitate the development of drug-resistant cancer cell clones or induce mutations of enzymes involved in relevant metabolic pathways [1].

Ibrutinib, Idelalisib and Venetoclax are the most common targeted chemo therapy drugs administered during the progression of Chronic Lymphocytic Leukemia. These drugs specifically target the B-cell receptor signaling pathway or the B-cell lymphoma two family of proteins. These group of proteins are encoded by the BCL2 gene and regulate cell death via transcriptional regulation, inducing or inhibiting apoptosis. The family is structurally divided into three distinct groups based on the presence of Bcl-2 homology (BH) domains (BH1-4). Chemo drugs suppress the alternative pathways these proteins can take since overexpression of the antiapoptotic BCL2 proteins lead to cell proliferation and various immunotherapies will attack the prosurvival BCL2 family proteins. [7].

1.1 Prior Models

In a 2014 study, Komarova and colleagues used stochastic models to study the evolution of ibrutinib resistance in CLL. The overall aim of the study was to model the evolutionary dynamics of ibrutinib-resistant mutations in the absence and presence of ibrutinib therapy [2]. Ibrutinib is a type of targeted therapy for CLL; however, some patients become resistant to the therapy [2]. This paper seeks to improve the understanding of the mechanism behind the formation of ibrutinib resistant mutations that lead to therapeutic resistance. A stochastic continuous time birth-death process is used to model the growth of the CLL cells as well as the probability of developing resistant mutations [2]. The authors assume the CLL cells grows exponentially; however, other studies have found that the CLL cells grow logistically for some patients [2][3]. Additionally, the model assumes that from a single cell a colony of cancer cells grows stochastically and with each cell division there is a small probability of developing a resistant mutation [2]. Furthermore, it assumes the mutation rate of each mutation is 10^{-8} [2]. To model the mutant growth, a stochastic model was used until the resistant cells reached a size of 1000 cells and then the model switched to a deterministic model to reduce computational time [2]. Both clinical data and realistic parameter combinations were used [2].

One of their most prominent discoveries is that drug-resistant CLL are present before treatment begins. In addition, these authors suggest that resistance mutations may have a selective advantage as large as 1.5% in the absence of treatment, although they are unable to exclude the possibility of no selective advantage. Additionally, at the time of treatment and even 300 days after treatment is initiated, the number of resistant mutations is very small and resistance is not immediately detectable. There is great variation in the development of resistance between patients after treatment begins. The average time of developing resistance after treatment initiation is 9 years if it is assumed a neutral selective advantage of the resistant mutations [2]. Given that 1.5% selective advantage is accounted, then the average time of developing resistance is 5 years [2]. The heterogeneity of the dynamics of resistance growth is more strongly correlated with the differences in the net growth rates of CLL cells rather than the tumor size at the beginning of therapy. Despite the great variation in the cellular growth dynamics across patients, the expected time until relapse is a reliable indicator of how long ibrutinib is effective at controlling the disease. The authors proposed that combining different kinase inhibitors with ibrutinib could prevent disease progression due to resistant mutations [2].

In recent years, it has been shown that CLL exhibits different growth profiles in different patients. In a 2019 study, Gruber et al. found that CLL can undergo exponential growth in some patients, but logistic growth in others [3]. In order to demonstrate this they used serial samples collected from 21 patients before therapy and then they corroborated their results in 86 independent patients with CLL [3]. Then they undertook an integrative analysis of genetic data, clinical information, and growth dynamics, including quantification of the effect of cancer mutation on growth rates measured in serial samples. The cohort was balanced for the strong prognostic marker of the mutational status of the IGH variable region (IGHV), they then evaluated the overall growth of the leukemia in each patient by examining between 4 and 83 pre-treatment measurements of peripheral white blood cell (WBC) counts per patient. It was found that a subset of patients exhibited bounded growth, with WBC counts plateauing overtime suggesting that leukemia can display logistic-like behavior as well as an exponential-like growth pattern. In order to estimate the posterior probabilities of the growth rate (r) and carrying capacity (K) they used a Markov Chain Monte Carlo (MCMC) Gibbs sampler. They found that of 106 patients, 48 had logistic growth profiles, 35 had indeterminate growth profiles and 22 had exponential growth profiles. Patients with exponential growth profiles tended to harbor more driver mutations than those with logistic or indeterminate profiles. Logistic tumors were more likely to have a mutated IGHV gene than exponential tumors.

2 Research Objectives

We will explore two main questions as well as a variety of sub-questions. First, We will analyze the impact of density dependence on the accumulation of resistance mutations in our model. The paper by Komarova et al. assumes that CLL cells grow exponentially [2]. We will analyze the impact of implementing density dependence in the per capita birth rate of the CLL cells and compare our model to the Komarova model. Additionally, we will explore how restricting the birth rate to model density dependence affects the overall growth of the number of resistant mutations that emerge. Since many of the previous models did not account for density dependence, incorporating such a factor could resemble a more robust model since tumors in cancer are largely dependent on the extracellular environment and have real life limitations. Also, we are interested in analyzing the role of density dependence on how often resistant sub-clones develop since the sub-clones help drive the formation of the mutations. Sub-clones are varying cell populations of the heterogenic tumor which encompass a reservoir of mutant cells that can expand, repopulate the tumor, and result in the rapid emergence of resistance. Due to the profound effect of these sub-clones, the density dependence is a necessary factor to investigate in our model.

Additionally, we will explore the impact of variation in our input parameters effect treatment duration. Previous research has assumed the the mutant cells were completely resistant to treatment [2]. Furthermore, we will examine the impact of partial resistance on the treatment duration. If mutant cells are partially sensitive to treatment, then treatment may be effective for a longer duration of time. In addition, we will study how the timing of the onset of treatment impact the duration of effective treatment. Furthermore, we will investigate the impact of the mutation rate to analyze the extent of the impact of a higher mutation rate on effective treatment duration. In summary, our questions are as follows:

1. How does density-dependence of tumor growth impact the evolution of drug resistance in CLL?
    (a) What impact does density-dependence have on the total size of the population of resistant mutations?
    (b) What impact does density-dependence have on the relative frequencies of resistant sub-clones?
2. How does variation in different parameters effect treatment duration?
    (a) What is the impact of variation in susceptibility to chemotherapy?
    (b) What is the impact of variation in time of treatment initiation?
    (c) What is the impact of variation in mutation rate?

3 Methods

In order to explore the questions raised above, we formulated a discrete time stochastic model for the growth of a tumor with mutation from drug-sensitive to drug resistant phenotypes. The original continuous-time model studied by Komarova et al. is a birth-death process, meaning that only one cell can divide or die at a time [2]. However, in our model, many events can happen in a single time step and so we are not working with a birth-death process. The model incorporates density dependence as well as treatment. The following subsections will discuss the model in more depth. The code for the model is located in the Appendix.

3.1 Model Description

3.1.1 Discrete Time

To reduce the time required for simulations, we opted to work with a discrete-time stochastic process rather than a continuous-time process. We are using discrete time which means we need to specify a time step ($tstep$). Our time step is $\frac{1}{4}$ which corresponds to 6 hours. Discussion about validating the time step can be found in a later section.

3.1.2 Density Dependence

Density dependence is incorporated in the model by assuming the per-capita birth rate b of the sensitive (sen) and mutant (mut) cells is density-dependent. In the absence of treatment, we assume the per-capita birth rate of the sensitive and mutant cells is the same. Therefore, we assume the following:

$$b(N) = \frac{b}{1 + CN}$$

where C controls the strength of the density dependence and N is the total number of sensitive and resistant (mutant) cells at that time. Our per-capita death rate d is held constant. The population of cancer cells tends towards a stable equilibrium size K, where the per-capita birth and death rates are equal. Setting $b(K) = d(K)$, we can then solve for K, which is:

$$\begin{aligned} b(K) &= d(K) \\ \frac{b}{1 + CK} &= d \\ K &= \frac{b - d}{dC} \end{aligned}$$

We allow the user to input the carrying capacity K; therefore, we calculate the corresponding C value which is as follows:

$$C = \frac{b - d}{dK}$$

3.1.3 Parameter Estimates

Our model contains various input parameters. A brief description of the input parameters are displayed in Table 1. In the table "SC" refers to sensitive cells and "MC" refers to the mutant cells. Also, the units of the parameters n_{detect}, n_{treat} , and n_{fail} refer to the total number of cells (mutant and sensitive cells). It is to be noted that many of these parameters were based on the values used in the Komarova et al. (2014) paper.

Parameter	Description	Units	Value	Reference
n_{detect}	Detection level	$cells$	10^{10}	[2]
n_{treat}	Treatment level	$cells$	$[10^{10} - 10^{12}]$	[2]
n_{fail}	Treatment failure level	$cells$	$1.01 \times n_{treat}$	[2]
b_{sen}	Sensitive cell birth rate	$days^{-1}$	$[0.0022, 0.004, 0.01777]$	[2]
d_{sen}	Sensitive cell death rate	$days^{-1}$	$[0.0013, 0.0024, 0.01056]$	[2]
K_{sen}	SC carrying capacity (before treatment)	$cells$	$[10^5 - 10^{14}]$	[2] [3]
$K_{plateau}$	SC carrying capacity (after treatment)	cells	10^9	[2]
b_{mut}	Mutant cell birth rate	$days^{-1}$	$[0.0022, 0.004, 0.01777]$	[2]
d_{mut}	Mutant cell death rate	$days^{-1}$	$[0.0013, 0.0024, 0.01056]$	[2]
K_{mut}	MC carrying capacity (before treatment)	$cells$	$[10^5 - 10^{14}]$	[2] [3]
μ	Mutation rate	$\frac{mutations}{cell\ division}$	$[10^{-6} - 10^{-8}]$	[2]
res	Level of resistance of mutant cells	NA	[0-1]	

Table 1: Input Parameters

3.2 Model

We begin our model starting from one sensitive cell and zero mutant cells. For each time step in the model, we calculate the number of births and deaths of sensitive and mutant cells as well as mutations. We assume that the number of events of each type (births, deaths and mutations) is Poisson-distributed. This assumption is justified by the law of rare events provided that the (1) number of cells is large (e.g., greater than 25), (2) that the per-capita probability of each event is small (e.g., less than 0.1), and (3) that each cell divides, dies or mutates independently of the others. We represent the number of sensitive cells as s and the number of mutant cells as m. In

the absence of treatment, we calculate the following variables to determine the population size of the sensitive and mutant cells. We incorporate density dependence for the sensitive and mutant cells as follows:

$$brate_{sen} = \frac{b_{sen}}{1 + C_{sen}(s + m)}$$
$$brate_{mut} = \frac{b_{mut}}{1 + C_{mut}(s + m)}$$

Then we compute the number of births and deaths for the sensitive and mutant cells, as well as the number of mutations using a Poisson distribution. We assume that mutations occur only during cell division and that each dividing sensitive cell mutates to a resistant phenotype with probability μ.

$$\begin{aligned} births_{sen} &\sim \text{Poisson}(s \times brate_{sen}) \\ deaths_{sen} &\sim \text{Poisson}(s \times d_{sen}) \\ mutations &\sim \text{Poisson}(births_{sen} \times \mu) \\ births_{mut} &\sim \text{Poisson}(m \times brate_{mut}) \\ deaths_{mut} &\sim \text{Poisson}(m \times d_{mut}) \end{aligned}$$

After each time step, we update the sizes of the sensitive and mutant cell populations using the following recursive equations:

$$\begin{aligned} s' &= s + births_{sen} - deaths_{sen} - mutations \\ m' &= m + births_{mut} - deaths_{mut} + mutations \end{aligned}$$

Treatment is initiated once the total population of sensitive and mutant cells exceeds the threshold n_{treat}. Treatment causes a reduction in the maximal sensitive cell division rate which drives the population of resistance cells towards a lower stable equilibrium denoted as $K_{plateau}$. Therefore, we must account for the new carrying capacity in the birth rate of the sensitive cells which we will denote as $b_{sen|treat}$. We know that $K = (b-d)/dC$, so we substitute in our new variables and solve for $b_{sen|treat}$ which gives us:

$$b_{sen|treat} = d_{sen} \times C_{sen} \times K_{plateau} + d_{sen}$$

Previous research has assumed that mutant cells are completely resistant to treatment. However, we want to explore varying levels of resistance of the mutant cells so during treatment we define the birthrate of mutant cells as:

$$b_{mut|treat} = res \times b_{mut}$$

Where res can vary from 0 to 1 and $res = 1$ corresponds to complete resistance. Therefore, our new birth rates during treatment are as follows:

$$\begin{aligned} b_{sen|treat} &= d_{sen} \times C_{sen} \times K_{plateau} + d_{sen} \\ b_{mut|treat} &= res \times b_{mut} \end{aligned}$$

Now we incorporate density dependence as follows:

$$\begin{aligned} brate_{sen|treat} &= \frac{b_{sen|treat}}{1 + C_{sen}(s+m)} \\ brate_{mut|treat} &= \frac{b_{mut|treat}}{1 + C_{mut}(s+m)} \end{aligned}$$

Then the number of births, deaths, and mutations occurring during treatment are:

$$\begin{aligned} births_{sen} &\sim \text{Poisson}(s \times brate_{sen|treat}) \\ deaths_{sen} &\sim \text{Poisson}(s \times d_{sen|treat}) \\ mutations &\sim \text{Poisson}(births_{sen|treat} \times \mu) \\ births_{mut} &\sim \text{Poisson}(m \times brate_{mut|treat}) \\ deaths_{mut} &\sim \text{Poisson}(m \times d_{mut|treat}) \end{aligned}$$

Similarly, as before we update our sensitive and mutant population sizes. The total population of cells initially decreases due to treatment and then increases due to an accumulation of mutant cells which are resistant to treatment. We continue treatment until the total cell population exceeds a threshold n_{fail}. In general, n_{fail} was set equal to $1.01 \times n_{treat}$, so that treatment is deemed to have failed when the population of tumor cells slightly exceeds the threshold at which treatment is initiated.

3.3 Summary Statistics

We report different summary statistics relating to time and the number of mutant cells to conduct our analysis. We calculate the median, mean, and standard deviation of detection time which occurs until the total cell population exceeds a threshold n_{detect}. We report the same statistics for the time of treatment failure which occurs when the total population of cells exceeds $1.01 \times n_{treat}$

after treatment begins. We calculate the duration of effective treatment by taking the difference of the time elapsed from treatment initiation to treatment failure, and likewise we report the same statistics as above. For the mutant cell population we report the same statistics as above; however, because the distribution of the number of mutant cells is highly skewed we also reported the following quantiles: $10\%, 25\%, 75\%, 90\%$. We determine the mutant population at the time of detection and treatment initiation.

3.4 Approximations

To reduce the time required to simulate this model, we approximated the Poisson distribution by its mean whenever the mean exceeded a specific threshold. For each time step we generate the number of birth and death events for sensitive and mutant cells as well as mutation events. We define a function called *mpoiss* which is a hybrid Poisson random number generator and our threshold value is 1000. For each type of event, we input the mean number of events. In the case that the mean is less than 1000 (our threshold), we simulate a random number from a Poisson distribution with our specified mean to determine the number of events that occur. Given the case that the mean is greater than or equal to 1000 then we use a deterministic approximation where the number of events is equal to the mean.

4 Results

4.1 Illustration of our Model

We are starting with a discrete time model that uses a hybrid deterministic Poisson generator. In Figure 1, we plot the sample paths for 20 independent simulations of the model. Figure 1a shows the sensitive cell population over time, while Figure 1b shows the mutant cell population over time. The parameter values used for these simulations are as follows: $b_{sen} = .004$, $d_{sen} = .0024$, $K_{sen} = 10^6$, $b_{mut} = 0.0029$, $d_{mut} = 0.0026$, $K_{mut} = 10^6$, $\mu = 0.000001$.

Figure 2 shows a visual illustration of our model that includes treatment. The solid blue line represents the total population of sensitive and mutant cells. We can see that once the total cell population reaches the treatment level threshold that the total cell population initially decreases due to treatment and then increase due to an accumulation of mutant cells. The parameters combination for this graph is as follows: $n_{detect} = 10^{10}, n_{treat} = 8 \times 10^{12}, n_{fail} = 8.08 \times 10^{12}, b_{sen} = 0.004, d_{sen} = 0.0024, K_{sen} = 10^{14}, K_{plateau} = 10^9, \mu = 10^{-8}, b_{mut} = 0.004, d_{mut} = 0.0024, K_{mut} = 10^{14}, res = 1$.

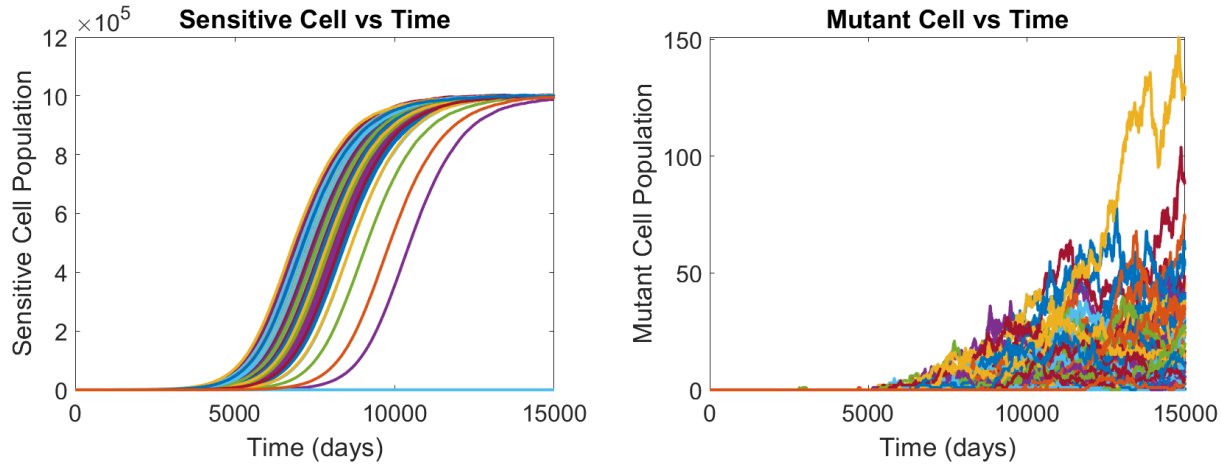

(a) (b)

Figure 1

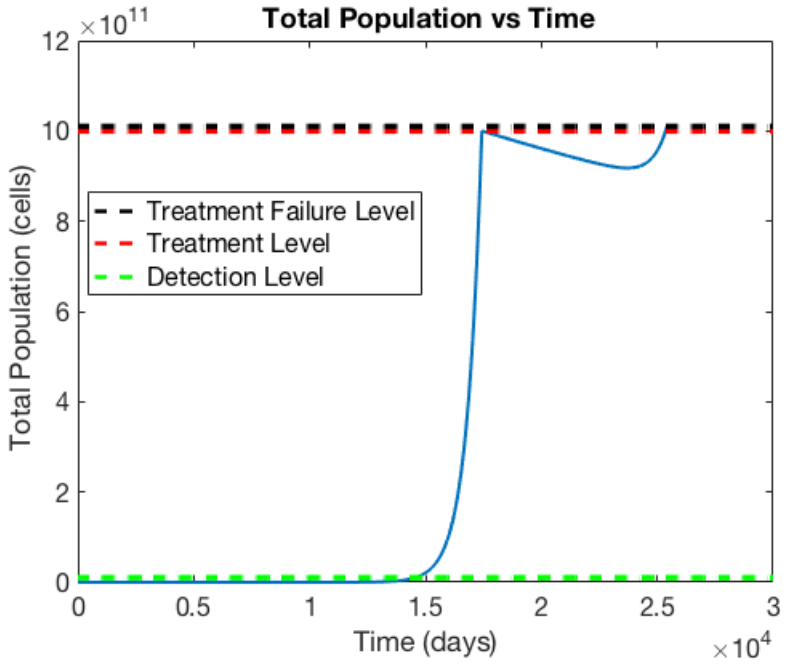

Figure 2

4.2 Numerical Approximations

4.2.1 Impact of Discretization of Time on Model Dynamics

We wanted to investigate the impact of the size of the time-step on the dynamics of our sensitive and mutant populations. To achieve this, we varied the size of the time step from 1 hour to 19 hours. For each such value, we ran 50 simulations, starting with an initial population containing

10 sensitive cells and 0 mutant cells and lasting 10,000 days. The values of the remaining model parameters were birth rate of sensitive type (b_{sen}) = 4×10^{-3}, death-rate of sensitive type (d_{sen}) = $0.6 \times 4 \times 10^{-3}$, birth rate of mutant type (b_{mut}) = 10^{-4}, death rate of mutant type (d_{mut}) = 10^{-5}, carrying capacity of mutant type (K_{mut}) = 10^{10}, carrying capacity of sensitive type (K_{sen}) = 10^{12} and mutation rate (μ) = 10^{-7}. We then plotted the mean sensitive cell population and mean mutant cell population at the final step (See Figure 3).The plots suggest that the behavior of the model is not strongly impacted by the size of the time step, at least within the range considered as the error bars overlap. A time-step of about 6 hours is chosen for our model input as it is appropriate to give us accurate results and because it is computationally faster.

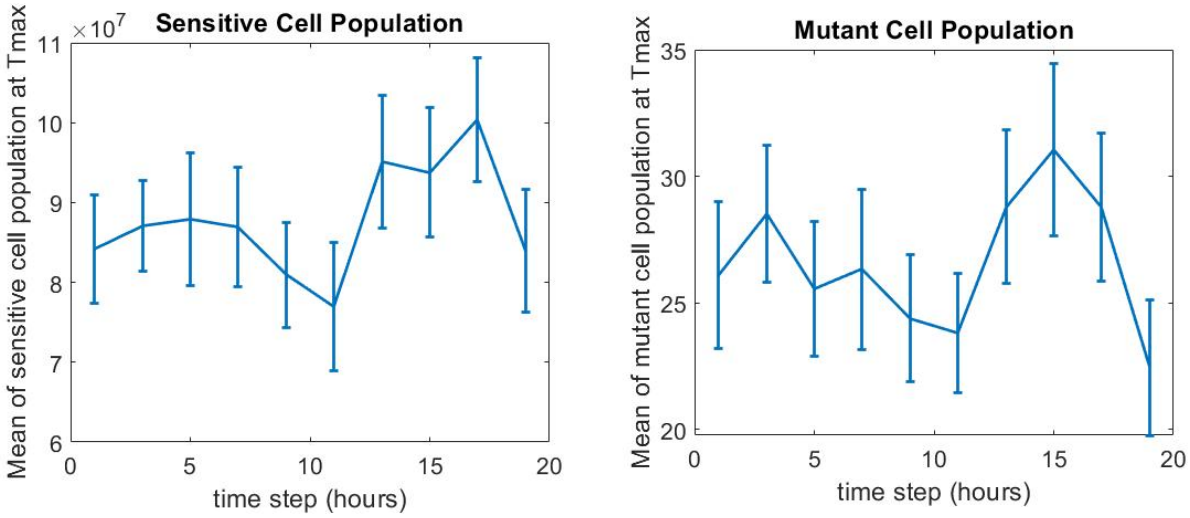

(a) (b)

Figure 3

4.2.2 Impact of Deterministic Approximation

One of the technical things that have to be tested is the effect of the deterministic approximation. To do this, we ran several sets of approximations using different values for the threshold above which the Poisson distribution was replaced by its mean. Setting this threshold equal to 0 gives a fully deterministic model, whereas setting this threshold equal to infinity gives a fully stochastic model. The function looks at the argument and if the argument is less than the threshold that it simulates a Poisson distributed random variable with that mean. If the mean value its greater than the threshold then it just assumes the random variable to mean. The way we have been approximating it is by keeping all the values in the simulation fixed and changing the value of the threshold to see the behavior of the simulation by comparing the mean and the standard deviation of the population of sensitive cells and mutant cells. We ran two independent sets of

simulations with each threshold value and then we plotted the mean with the standard deviation of the numbers of sensitive and mutant cells at time $t = T_{max}$. The threshold was varied between 10^2 to 10^{10} and this process was repeated twice. In figure 4 the distributions of sensitive and mutant cells did not appear to be strongly affected by the threshold used so we will use a value of 10^3 for our future simulations. The parameters we used are: $S_0 = 10$, $M_0 = 0$, $b_{sen} = 4x10^{-3}$, $d_{sen} = 2.4\times10^{-3}$, $K_{sen} = 10^5$, $b_{mut} = 2.9\times10^{-3}$, $d_{mut} = 2.6\times10^{-3}$, $K_{mut} = 10^5$, $\mu = 10^{-6}$.

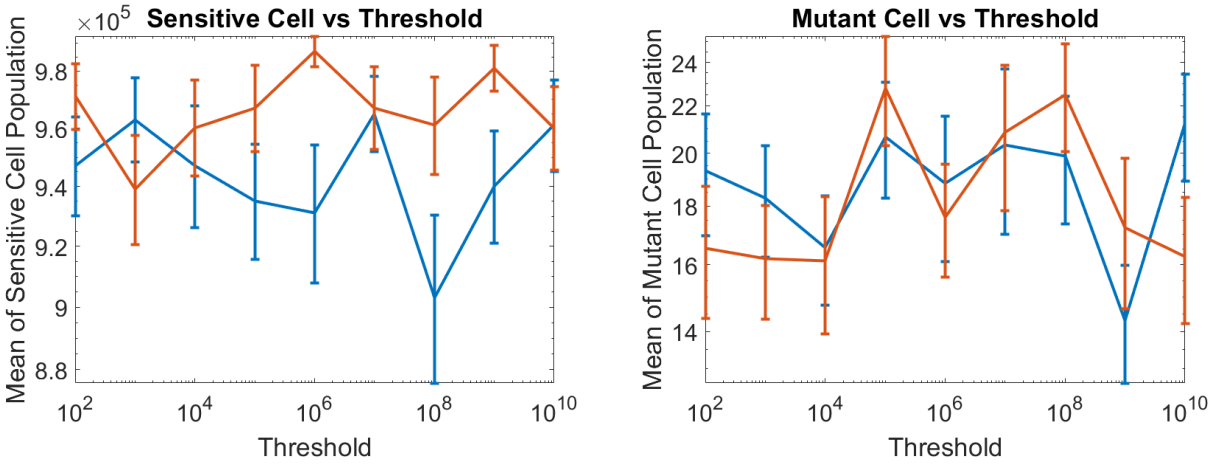

(a) (b)

Figure 4

4.3 Dynamics of Sensitive and Resistant Cells under Treatment

4.3.1 Density-Dependent Cell Division

In this experiment we aim to investigate the impact carrying capacity (K_{sen}) has on the mean duration of effective treatment as well as on the number of resistant cells at the onset of treatment. To achieve this, we varied K_{sen} between 10^{13} and 10^{16} while the other model parameters were kept fixed. When K_{sen} is very large (e.g.10^{16}), the cell growth dynamics are approximately exponential. We ran a 100 simulations were run for each K_{sen} and two sets of fixed parameters corresponding to slow and fast growing tumors. The initial number of sensitive cells (S_0) was set to be 1 while the initial number of mutant cells (M_0) was set to be 0, and the simulations were allowed to run for a maximum time (T_{max}) of 50,000 days. Further on, to investigate an additional impact of mutation rate (μ), two different values of μ were used which were 10^{-8} and 10^{-7}. The summary statistics were then plotted for both fast and slow growing tumors (See Figures 5,6).

The parameter values used for slow growing tumors are $n_{detect} = 10^{10}$, $n_{treat} = 8 \times 10^{12}$, $n_{fail} = 1.01 \times n_{treat}$, $b_{sen} = 0.004$, $d_{sen} = 0.0024$, $K_{plateau} = 10^9$, $\mu = 10^{-8}/10^{-7}$, $b_{mut} = 0.004$, $d_{mut} = 0.0024$, $res = 1$ $K_{mut} = K_{sen}$. And, the parameter values used for fast growing tumors are $n_{detect} = 10^{10}$, $n_{treat} = 8 \times 10^{12}$, $n_{fail} = 1.01 \times n_{treat}$, $b_{sen} = 0.01777$, $d_{sen} = 0.01056$, $K_{plateau} = 10^9$, $\mu = 10^{-8}/10^{-7}$, $b_{mut} = 0.01777$, $d_{mut} = 0.01056$, $res = 1$, $K_{mut} = K_{sen}$. It is to be noted that $b_{sen} = b_{mut}$, $d_{sen} = d_{mut}$ and $K_{sen} = K_{mut}$ before the treatment is started.

It is observed that as K_{sen} increases, the mean duration of effective treatment decreases in both slow and fast growing tumors. This is because, as we increase K_{sen}, we are allowing for higher densities of mutant hence resistant cells to divide more rapidly, thus the treatment fails faster or the mean duration for effective treatment decreases. A higher mean duration of effective treatment is also noticed in slow growing tumors as compared to fast growing tumors for each value of K_{sen}. This is because, the demographic parameter ($r = b - d$) which determines the rate at which the resistant cells grow is equal to 1.6×10^{-3} and $7.2 \times 10{-}3$ for slow and fast growing tumors respectively. Since the value of r is higher in fast growing tumors as compared to the slow growing tumors, the mutant cells grow faster. As a result, the mean duration of effective treatment is smaller.

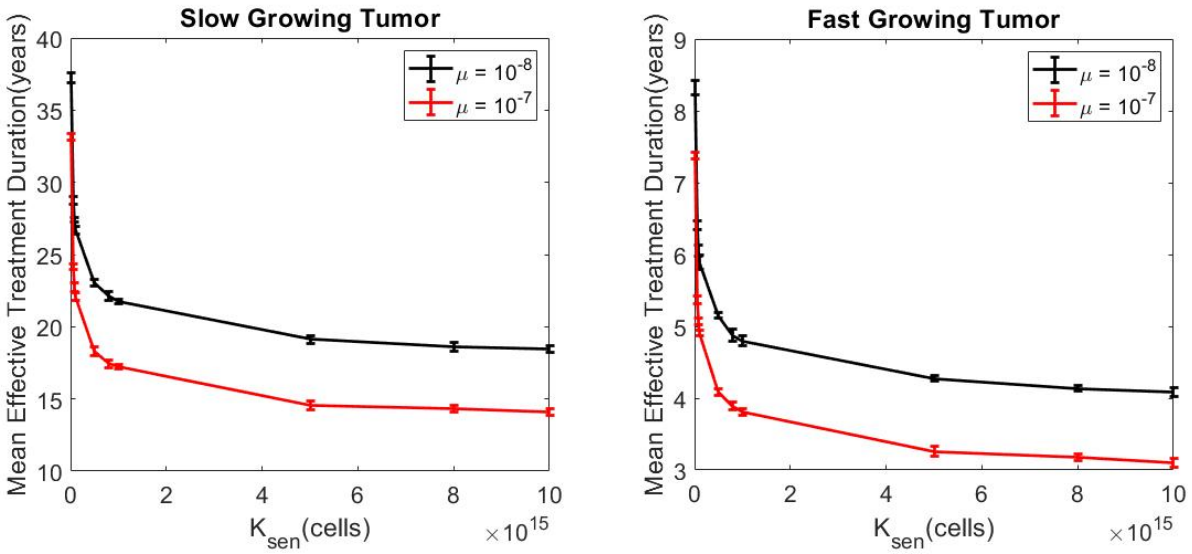

(a) (b)

Figure 5

Additionally, a lower mean duration of effective treatment is observed for a higher mutation rate (10^{-7}) as compared to the lower (10^{-8}) for both fast and slow growing tumors as a higher mutation rate implies a faster growth of mutant cells thus causing a decrease in the mean duration of effective treatment. It is also observed that the number of mutant cells at the time of the onset

of treatment is not significantly impacted by the carrying capacity for both mutation rates and in both fast and slow growing tumors as the number of mutant cells at the onset of treatment depends on the number of cell divisions that have occurred by that time. However, in the current model, treatment begins once the total population size exceeds a set threshold, $n_{treat} = 8 \times 10^{12}$, and so the number of cell divisions by this time will not be strongly influenced by the carrying capacity.

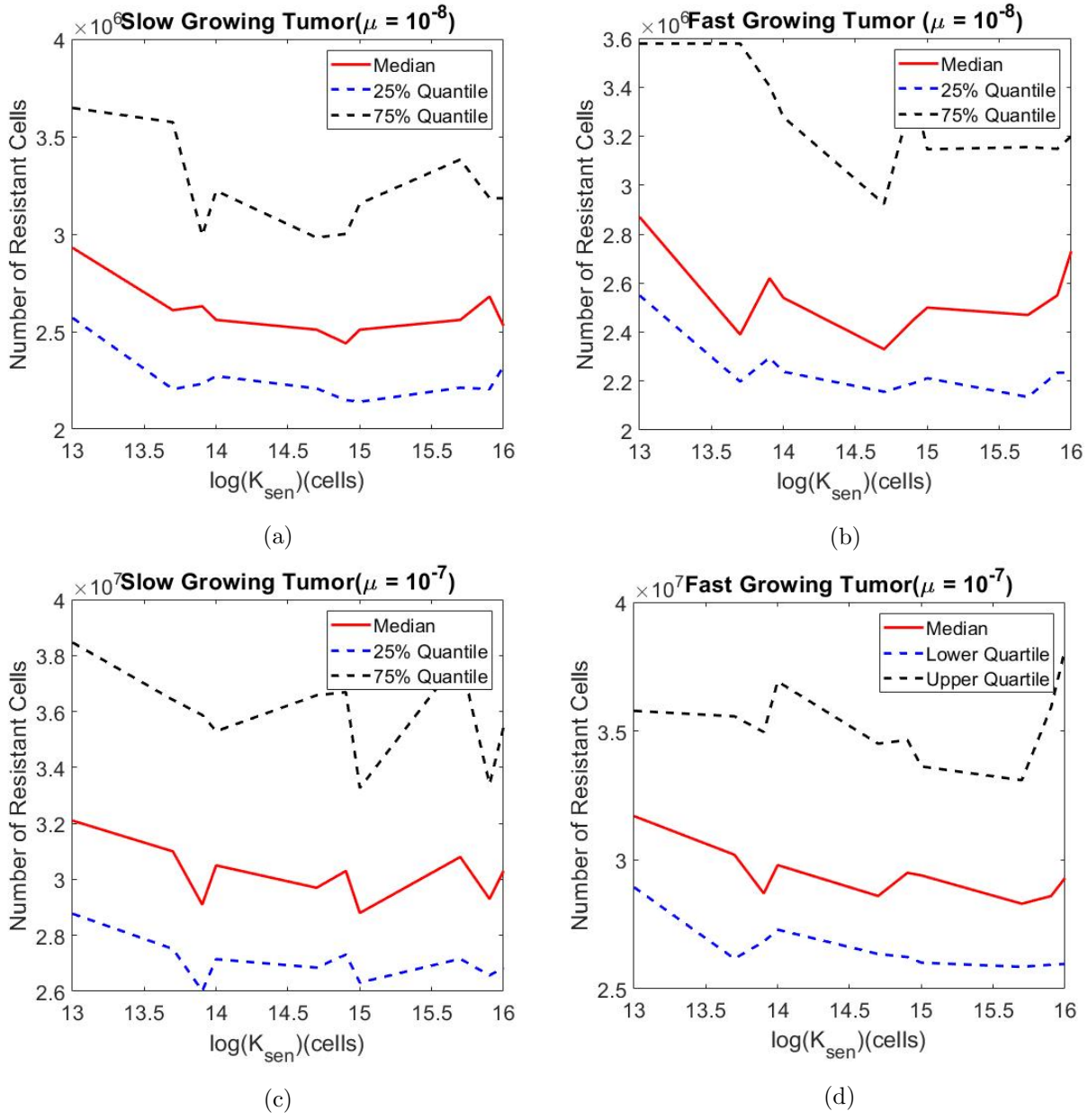

Figure 6

4.3.2 Partial Resistance

In the model studied by Komarova et al. (2014), it is assumed that mutant cells are completely resistant to treatment [2]. We explore the impact of partial resistance of the mutant cells on the duration of effective treatment. Without treatment, the birth rate of the mutant cells is b_{mut}. We incorporate partial resistance during treatment by setting $b_{mut|treat}$ equal to $res \times b_{mut}$ where res is between zero and one inclusively. If $res = 1$, then the mutant cells are completely resistant as $b_{mut|treat} = b_{mut}$. We vary res between 0.70 to 1 in increments of 0.05 for different carrying capacities, K_{sen} and K_{mut}, where $K_{sen} = K_{mut}$ since we have no justification for the carrying capacities to differ in size. We examined varying resistance levels for the following carrying capacities: $5 \times 10^{13}, 10^{14}, 5 \times 10^{14}$, and 10^{15}. We chose this range of carrying capacities to analyze the impact of varying resistance levels on tumor growth that behaves logistically and exponentially. We ran 100 simulations for each level of resistance and carrying capacity. All of the other parameters were held fixed. For each of the parameter combinations the mean effective treatment duration as well as its standard deviation were reported. Figure 7 illustrates our findings. The fixed parameters in the model are as follows: $n_{detect} = 10^{10}, n_{treat} = 8 \times 10^{12}, n_{fail} = 8.08 \times 10^{12}, b_{sen} = 0.1777, d_{sen} = 0.01056, K_{plateau} = 10^{9}, \mu = 10^{-8}, b_{mut} = 0.1777, d_{mut} = 0.01056$. The specific birth and death rates for the sensitive and mutant cells were chosen because they correspond to a fast growing tumor which is more likely to result in treatment failure.

In Figure 7, we can see that an increase in the level of resistance results in a decrease in the mean of the duration of effective treatment, as would be expected as the mutant cells are able to grow more rapidly. Also, an increase in resistance level causes a decrease in variation of effective treatment duration for the different carrying capacities. If we assume complete resistance, then the mean duration of effect treatment is roughly between 4 to 6 years. However, if the mutant resistance level is lower than approximately 0.85, then the treatment is essentially effective. The median age of diagnosis is roughly 70 years [6]. If the effective treatment duration is greater than 10 years, then the treatment is essentially effective as the patient is more likely to die from other natural causes associated with their age. Furthermore, an increase in carrying capacity is associated with a shorter effective duration as the cell population is growing more rapidly. In conclusion, the carrying capacity of the sensitive and mutant cells has a greater impact at lower resistance levels. Also, a higher carrying capacity corresponds to a shorter duration of effective treatment. If a drug could be engineered to reduce the birth rate of the mutant cells during treatment by roughly 15%, then treatment could be deemed completely effective regardless of the carrying capacity of the tumor.

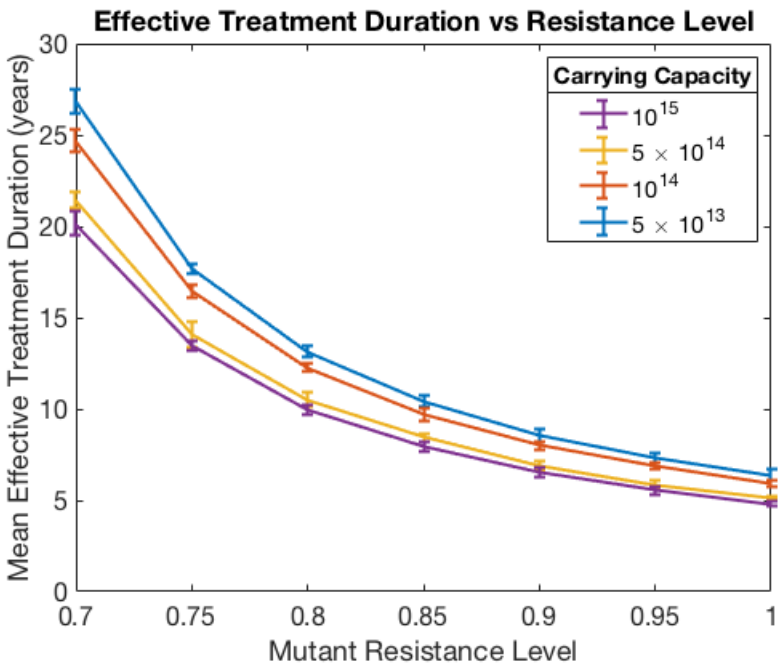

Figure 7

4.3.3 Treatment Initiation

In this experiment, we varied the size of the population of tumor cells (n_{treat}) at which treatment was initiated from 10^{10} (the limit of detectability) to 10^{12}. 100 simulations were conducted for each set of parameter values, either with $K = 10^{13}$ (logistic growth) or $K = 10^{15}$ (exponential growth). When the threshold for treatment initiation was increased, we saw an increase in the number of mutants at onset of treatment, duration of effective treatment, and treatment failure time when the number of tumor cells increased from 10^{10} to 10^{12}. When we changed the carrying capacity to account for an exponential growth model, we observed similar increases in these quantities.

After increasing the carrying capacity, there were some important trends to be noted. The detection time remained constant no matter the carrying capacity after increasing the population of tumor cells. However, treatment failure time increased when mutant population size increased only at carrying capacities $K = 10^{13}$ and $K = 3 \times 10^{13}$. With carrying capacities above this range, the treatment failure time decreased as the mutant population increased. In all simulations no matter the carrying capacity, the duration of effective treatment decreased as the tumor cell population increased which is as expected. The number of mutants at tumor detection decreased as tumor population increased for carrying capacities $K = 10^{13}$ and $K = 3 \times 10^{13}$. However, with greater carrying capacities, as the tumor cell population increased, the mutants at tumor detection increased.

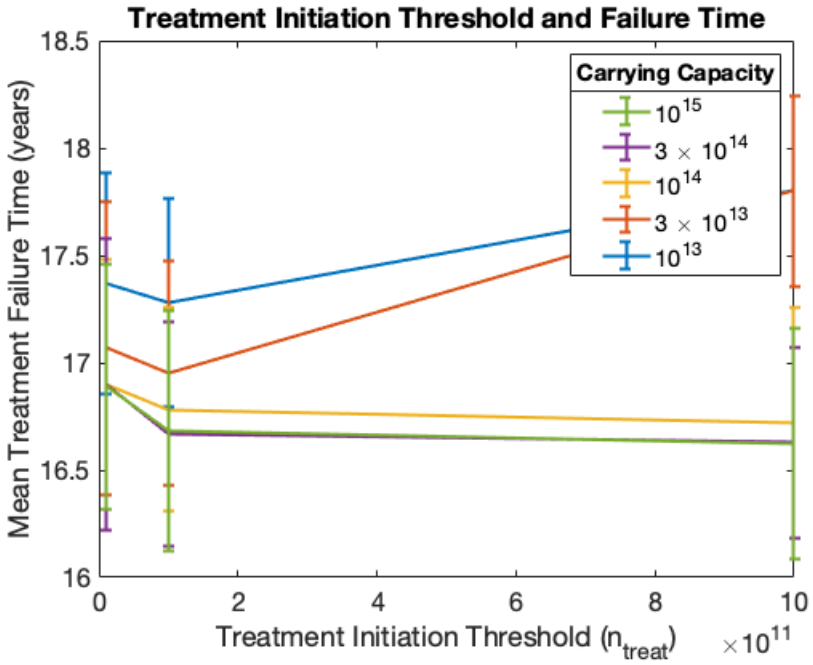

Figure 8

Throughout all carrying capacities, as the tumor cell population increased, the number of mutants at onset of treatment also increased. Therefore, the treatment failure time and the number of mutants at tumor detection differed in relationship with tumor cell population as the carrying capacity increased. We detail treatment failure time with Figure 8 and the duration of effective treatment time with Figure 9, as the tumor cell population increases for varying carrying capacities. The parameter values used were $n_{detect} = 10^{10}, n_{fail} = 5 \times 10^{12}, b_{sen} = 0.1777, d_{sen} = 0.01056, K_{plateau} = 10^9, b_{mut} = 0.1777, d_{mut} = 0.01056$.

At smaller carrying capacities such as $K = 10^{13}$ and $K = 3 \times 10^{13}$, delayed onset of treatment (achieved by taking larger values of n_{treat}) leads to a modest increase in the treatment failure time. In contrast, at higher carrying capacities, the effect of the treatment threshold on the treatment failure time is limited. This difference likely arises from the fact that when the carrying capacity is similar in magnitude to the treatment threshold ($K \sim n_{treat}$), density-dependence slows the growth of the population of resistant cells in the period just prior to the onset of treatment.

In contrast, the mean duration of effective treatment appears to decrease as the treatment onset threshold increases. At low carrying capacities, this decrease reaches a plateau as n_{treat} approaches the carrying capacity. However, at higher carrying capacities, no such plateau was observed over the range of values of n_{treat} used in these simulations.

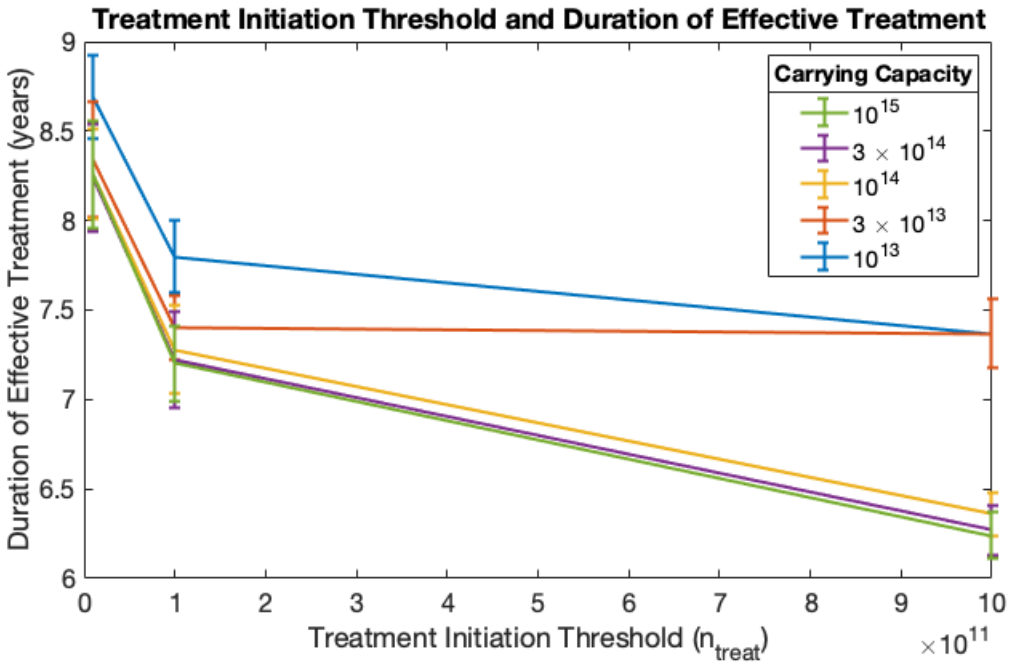

Figure 9

4.3.4 The Rate of Mutation to Resistant Phenotypes

We tested the impact of the mutation rate to resistant phenotypes. To do this we varied the mutation rate (to drug resistance) between 10^{-6} and 10^{-8} mutations/cell division. Biological differences in this rate can be due to variation in the intrinsic mutation rate as well as differences in the size of the mutational target for drug resistance. We conducted 100 simulations with the following set of parameter values: $n_{detect} = 10^{10}, n_{treat} = 8 \times 10^{12}, n_{fail} = 8.08 \times 10^{12}, b_{sen} = 0.1777, d_{sen} = 0.01056, K_{plateau} = 10^9, b_{mut} = 0.1777, d_{mut} = 0.01056$.

After varying the mutation rate the mean and standard deviation of the effective treatment duration was plotted against the mutation rate in a log-log plot in Figure 10. From the graph we could notice that this gives us a linear relationship where as we increased the mutation rate the number of years where the treatment is effective decreases. This relationship was expected because when we increase the mutation rate that increases the number of mutant cells at each change in the time step.

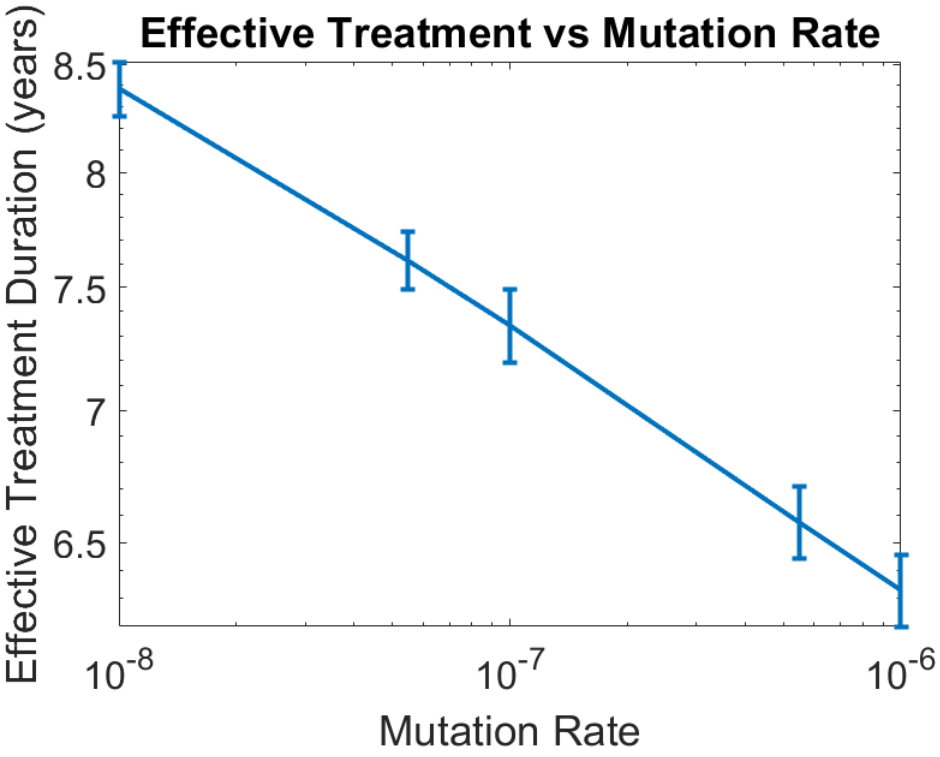

Figure 10

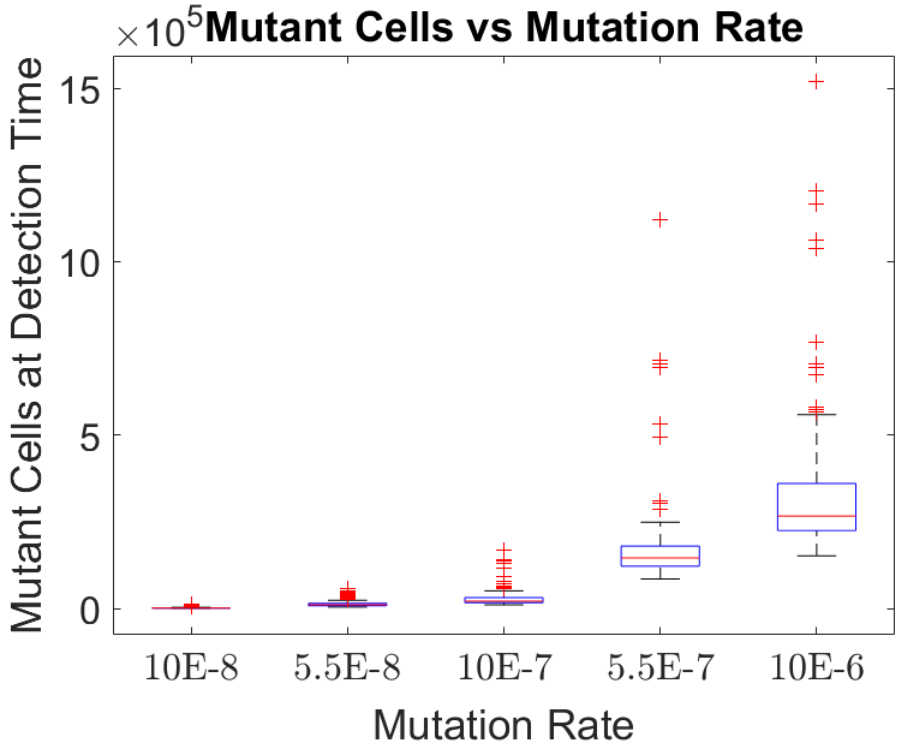

Figure 11

In Figure 11 we have five boxplots that represent the five different values of mutation rates that we used to run the simulations. We plotted the number of mutant cells at the detection time against the mutation rate and we used boxplot to represent this data. The reason we used boxplots is because this data is not normally distributed but instead is skewed so the median is a more robust parameter than the mean. From Figure 11 we can see that the median number of mutant cells at the detection time increases as the mutation rate increases.

5 Discussion

Individuals with CLL are currently facing issues with developing therapeutic resistance due to the accumulation of drug resistant mutations. Previous research has studied the the evolutionary dynamics of drug resistant mutations [2]. Additionally, prior research has investigated varying tumor growth dynamics in patients with CLL ranging from logistic to exponential growth [2] [3]. We developed a discrete time stochastic model to further analyze the dynamics of sensitive and resistant cells during treatment.

We have expanded upon the Komarova et al. (2014) proposed model by including density dependence in the growth of both sensitive and resistant cells instead of assuming exponential growth [2]. The impact of the carrying capacity on the dynamics of both sensitive and resistant tumor cells is investigated by simulation of the modified model using different values of K_{sen} for slow and rapidly dividing cancer cells and for different mutation rates.There have been some insightful observations. An increase in K_{sen} results in a decrease in the mean duration of effective treatment as this allows for higher densities of resistant cells to divide more rapidly, thus the treatment fails more rapidly. Additionally, it is observed that a higher mean duration of effective treatment is associated with slow growing tumors as compared to fast growing tumors for each value of K_{sen} as the value of $r = b - d$ is higher in fast growing tumors as compared to the slow growing tumors hence the resistant cells grow faster. Also, a lower mean duration of effective treatment is noted for a higher mutation rate as compared to the lower for both fast and slow growing tumors as a higher mutation rate implies a faster growth of mutant cells thus causing a decrease in the mean duration of effective treatment. Hence, density dependence does play an important role in the effectiveness of treatment thus should be included in treatment models.

Additionally, we expanded on Komarova et al. (2014) proposed model, to account for partial resistance of the mutant cells to treatment, instead of assuming complete resistance [2]. Through analyzing the impact of partial resistance of the mutant cells we discovered some interesting key findings. Higher resistance levels correspond to shorter mean duration of effective treatment, as the mutant cells are able to grow more rapidly. Also, larger carrying capacities are associated with a

shorter mean duration of effective treatment. Furthermore, the size of the carrying capacity has a larger impact at lower resistance levels. If we assume complete resistance, then the mean duration of effect treatment is roughly between 4 to 6 years. Whereas, if the mutant resistance level is below approximately 0.85, then treatment is essentially effective. Hence, partial resistance plays a significant role in the effectiveness of treatment regardless of the growth dynamics of the tumor cells. Future treatment methods should explore different methods of reducing the birth rate of the mutant cells so they are not completely resistant to treatment.

The size of the cancer cell population at the onset of treatment also impacts the dynamics of the resistant cell population. To investigate this relationship, the size of the population of tumor cells (n_{treat}) at which treatment was initiated was varied from 10^{10} (the limit of detectability) to 10^{12}. Furthermore, these simulations were carried out under different carrying capacities, ranging from $K = 10^{13}$ (logistic growth) to $K = 10^{15}$ (exponential growth). The parameter measurements showed interesting relationships which offers insight into the biological aspect of our model. We noted that when the carrying capacity was similar in magnitude to the treatment threshold, the resistant cells stalled in growth prior to the onset of treatment. It is unclear how often this situation occurs in reality, but the diversity of growth profiles documented by Gruber et al. (2019) suggests that this situation is at least plausible. However, density dependent inhibition is a very probable case our model could apply to. This occurs when cells grow to a limited density and then growth becomes inhibited, possibly by cell-cell contacts. Therefore, our model could be applied to include the possibility of cell-cell contact as well as other spatial requirements.

To study resistant phenotypes, the mutation rate (to drug resistance) was varied between 10^{-6} and 10^{-8} mutations/cell division. In the Komarova et al. (2014) mutation rate model they used a range of mutation rate from 10^{-7} and 10^{-9}. They plotted in a log log scale the mutation rate against the probability of resistance generation and got a linear relationships. Similarly to their results we also get a linear relationship between the mutation rate and the effective treatment duration when we plot on a log-log scale. In the Komarova et al. (2014) they use histogram to showcase the mutant population size at the start of treatment and after 300 days of treatment, they use the mean as their parameter. In our Figure 11 we chose to use the median of the mutant cells at detection time because the distribution of this number is highly skewed due to the random time at which the first resistance mutation occurs and the initially exponential growth of this sub-population (density dependence only becomes important when the cell number is very large). Furthermore, we explore the mutant population at the detection time and how the mutation rate affects the size of the mutant cells. As expected our box plot showcases a almost exponential increased in the median number of mutant cells at detection time. Lastly by investigating the impact of the mutation rate on the effective treatment duration we know that a higher mutation rate has a big significant on

the amount of years the treatment is effective.

5.1 Limitations of the Model

Our model is mostly limited in how biologically accurate it is for CLL patients in terms of distinguishing between different types of mutations that are present in the CLL patients' genome. For example, in CLL patients, there could be various chromosomal alterations such as deletions of certain loci [8]. Additionally, biological regulators, inflammatory receptors, transcriptional and translational regulators, mRNA splicing, and cell cycle control all contribute to the genetic heterogeneity that our model does not encompass [8]. We ignore heterogeneity in both the sensitive and resistant cell population. In particular, we assume that all cells carry the same number of driver mutations and we assume that sensitive and resistant cells have identical phenotypes prior to treatment.

Different loci of the genome are subject to different mutation rates and this therefore would make our model more specific to what patients will encounter with the onset of CLL. One way to express an important aspect of these biological markers would be to extend our model to account for mutation classes within different loci of the genome. Point mutation classes such as silent, nonsense, missense, and frameshift mutations would represent a more specific numbering model to account for this. Epigenetics could also play a part in which transcriptional regulation has a large influence on what genes are expressed or turned off. Our treatment model could also encompass these biological changes to quantify a more rigorous and biologically relevant model for CLL treatment.

Differences in cellular growth patterns across patients can lead to much variation not described by our treatment model. Therefore, the detection time is limited and unlikely to contribute to the diagnosis of many different patients. In addition, ibrutinib may be a poor option of therapy when stronger chemotherapies could exist for the genome profile of the patient. Finally, our model assumes that density dependence is only present with our cell division rate but is currently not supported by the scientific literature to have a biological basis. Density dependence is an important aspect of our model that gave us logical results, but this could be refined to include a more rigorous and applicable model of testing.

6 Conclusion

We developed a discrete-time stochastic model to analyze the dynamics of therapeutic resistance in CLL. To make our model more realistic, we incorporated density dependence and investigated the effects of treatment for different tumor growth dynamics. We analyzed the impact of density-

dependent cell division, partial resistance, time of treatment initiation, and mutation rate. It was observed that these factors play a significant role in governing treatment. Hence, future work should continue to explore these areas in more depth.

7 Acknowledgments

We would like to thank the Quantitative Research for the Life and Social Sciences Program (QRLSSP) for this opportunity. Also, we would like to thank our advisor, Dr. Jay Taylor, for his constant guidance and support. Additionally, we would like to thanks to our graduate student mentors, Jordy Cevallos Chavez and Lucero Rodriguez Rodriguez for their various contributions. Finally, we would like to extend our thanks to the faculty and staff as well as anyone who helped make the QRLSSP program possible.

References

[1] Nikolaou M, Pavlopoulou A, Georgakilas AG, Kyrodimos E. The challenge of drug resistance in cancer treatment: a current overview. Clin Exp Metastasis. 2018 Apr;35(4):309-318.PMID:29799080.

[2] Komarova, NL, Burger JA, Wodarz D (2014). Evolution of ibrutinib resistance in chronic lymphocytic leukemia (CLL). Proc Natl Acad Sci USA 111(38):13906–13911.

[3] Gruber, M et. al. (2019). Growth dynamics in naturally progressing chronic lymphocytic leukaemia. Nature, 570:474-479.

[4] Guiéze, R, Wu C (2015). Genomic and epigenomic heterogeneity in chronic lymphocytic leukemia. Blood 126(4):445–453.

[5] Rai, Kanti R., and Preetesh Jain. "Chronic Lymphocytic Leukemia (CLL)—Then and Now." American Journal of Hematology, vol. 91, no. 3, WILEY, 2016, pp. 330–40, doi:10.1002/ajh.24282.

[6] Bosch F, Dalla-Favera R. Chronic lymphocytic leukaemia: from genetics to treatment. Nat Rev Clin Oncol. 2019 Nov;16(11):684-701. doi: 10.1038/s41571-019-0239-8. PMID: 31278397.

[7] Fatima, N., Crassini, K. R., Thurgood, L., Shen, Y., Christopherson, R. I., Kuss, B., Mulligan, S. P., & Best, O. G. (2020, May 11). Therapeutic approaches and drug-resistance in chronic lymphocytic leukaemia. Cancer Drug Resistance. https://cdrjournal.com/article/view/3439.

[8] Gaidano, Gianluca, and Davide Rossi. "The Mutational Landscape of Chronic Lymphocytic Leukemia and Its Impact on Prognosis and Treatment." Hematology. American Society of Hematology. Education Program, American Society of Hematology, 8 Dec. 2017, www.ncbi.nlm.nih.gov/pmc/articles/PMC6142556/.

8 Appendix

MATLAB Code

Simulations are run from the wrapper code and the main code performs the function.

8.1 Wrapper Code

```
% This code include treatment for 1 mutant class
% %%%%%%%%%%%%%%%%%%%%%%%%%%%%%%%%%%%%%%%%%%%%%%%%%%%%%%%%%%%%%%%%%%%%%%%%%%%%%%%%%%


% User input

Num_sims = input('Number of simulations: ');
% Tmax = input('Maximum duration of simulation (days): ');
% n_detect= input('Detection level (cells): ');
% n_treat=input('Treatment level (cells): ');
% S0 = input('Initial number of sensitive cells: ');
% bsen = input('Sensitive cell birth rate/day: ');
% dsen = input('Sensitive cell death rate/day: ');
% Ksen = input('Sensitive cell carrying capacity (before treatment): ')
    ;
% K_plateau=input('Sensitive cell carrying capacity (after treatment):
    ');
% M0 = input('Initial number of mutant cells: ');
% mu = input('Mutation rate/division: ');
% bmut = input('Mutant cell birth rate/day: ');
% dmut = input('Mutant cell death rate/day: ');
% Kmut = input('Mutant cell carrying capacity (before treatment): ');
% res = input('Level of resistance of mutant cells to treatment: ');



Tmax = 50000;
n_detect= 10^(10);
n_treat= 8 * 10^(12);
n_fail = 1.01*n_treat;    % Set n_fail slightly above n_treat
S0 = 1;
bsen=.01777;
dsen=.01056;
Ksen=5*10^(14);
K_plateau= 10^(9);
```

```
M0 = 0;
mu=10^(-8);
bmut=.01777;
dmut=.01056;
Kmut=5*10^(14);
res = .7;



%%%%%%%%%%%%%%%%%%%%%%%%%%%%%%%%%%%%%%%%%%%%%%%%%%%%%%%%%%%%%%%%%%%%%%%%%%%%%%%

% Convert time to simulation units

tstep = 1/4;     % each time step corresponds to 6 hours (1/4 day)
Tmax = floor(Tmax/tstep); % converts the Tmax to be in terms of the tstep
bsen = bsen*tstep;
dsen = dsen*tstep;
bmut = bmut*tstep;
dmut = dmut*tstep;


% Convert carrying capacities to density-dependence parameters


Csen = (bsen - dsen)/(dsen*Ksen);
Cmut = (bmut - dmut)/(dmut*Kmut);

% Adjust birthrates during treatment

bsen_treat= dsen*Csen*K_plateau + dsen;
bmut_treat = res*bmut;



```

```matlab
% %%%%%%%%%%%%%%%%%%%%%%%%%%%%%%%%%%%%%%%%%%%%%%%%%%%%%%%%%%%%%%%%%%%%%%%%%%%%

% Make matrices to place values in

S_pop = NaN(Num_sims, Tmax+1);
M_pop = NaN(Num_sims, Tmax+1);
Total_pop = NaN(Num_sims, Tmax+1);
detect_t = NaN(1,Num_sims);
detect_m = NaN(1,Num_sims);
treat_t = NaN(1,Num_sims);
treat_m = NaN(1,Num_sims);
final_t = NaN(1,Num_sims);
delta_t = NaN(1,Num_sims);


% %%%%%%%%%%%%%%%%%%%%%%%%%%%%%%%%%%%%%%%%%%%%%%%%%%%%%%%%%%%%%%%%%%%%%%%%%%%%


% Run for Num_sims Simulations



for i = 1:Num_sims
    [S, M, m_det, t_det , m_treat, t_treat, t_final, extinct_flag] = DT_treatment_Final(Tmax , n_detect , n_treat , n_fail, S0 , bsen , dsen , Csen , bsen_treat , M0 , mu , bmut , dmut , Cmut , bmut_treat);
    while extinct_flag==1 % If the pop goes extinct rerun the simulation
        [S, M, m_det, t_det , m_treat, t_treat, t_final, extinct_flag] = DT_treatment_Final(Tmax , n_detect , n_treat , n_fail, S0 , bsen , dsen , Csen , bsen_treat , M0 , mu , bmut , dmut , Cmut , bmut_treat);
```

```
            fprintf('Simulation Number: %d\n',i);
        end
        if extinct_flag==0
        S_pop(i,:) = S;
        M_pop(i,:) = M;
        Total_pop(i,:) = S + M;
        detect_t(i) = tstep*t_det; % convert the time back into days
        detect_m(i)= m_det;
        treat_t(i)=tstep*t_treat;  % convert the time back into days
        treat_m(i)=m_treat;
        final_t(i) = tstep*t_final; % convert the time back into days
        fprintf('Simulation Number: %d\n',i); % print the current simulation number
        end
end


time = 0:Tmax; % total time length
time = tstep.*time;     % convert integer time back into days


% %%%%%%%%%%%%%%%%%%%%%%%%%%%%%%%%%%%%%%%%%%%%%%%%%%%%%%%%%%%%%%%%%%%%%%%%%%%

% Find the duration of effective treatment
% Note: the "isnan" condition is just in case the n_fail by the end of the
% run

for i= 1: Num_sims
        if(isnan(treat_t(i))==0 && isnan(final_t(i))==0)
            delta_t(i)= final_t(i)-treat_t(i);
        end
end


```

```
%%%%%%%%%%%%%%%%%%%%%%%%%%%%%%%%%%%%%%%%%%%%%%%%%%%%%%%%%%%%%%%%%%%%%%%

% Determine the number of simulations that reach _ level

Sims_detect = length(detect_t) - sum(isnan(detect_t));
Sims_treat = length(treat_t) - sum(isnan(treat_t));
Sims_final = length(final_t) - sum(isnan(final_t));

%%%%%%%%%%%%%%%%%%%%%%%%%%%%%%%%%%%%%%%%%%%%%%%%%%%%%%%%%%%%%%%%%%%%%%%%


fprintf('\n\n');
fprintf('Statistics \n\n');

% Number of Simulations
fprintf('Number of Simulations that reach 1st Detection: %d\n', Sims_detect);
fprintf('Number of Simulations that reach treatment: %d\n', Sims_treat);
fprintf('Number of Simulations that reach treatment failure: %d\n', Sims_final);
fprintf('\n');

% Time Statistics

fprintf('Time Statistics \n\n');


% Detection Time

fprintf('Detection time (days) \n');
fprintf('Median detection time: %d\n',nanmedian(detect_t));
fprintf('Mean detection time: %d\n',nanmean(detect_t));
```

```
157 fprintf('SD detection time: %d\n',nanstd(detect_t));
158 fprintf('\n');
159
160 % Treatment Failure Time
161
162 fprintf('Treatment failure time (days) \n');
163 fprintf('Median treatment failure time: %d\n',nanmedian(final_t));
164 fprintf('Mean treatment failure time: %d\n',nanmean(final_t));
165 fprintf('SD treatment failure time: %d\n',nanstd(final_t));
166 fprintf('\n');
167
168 % Duration of Effective Treatment
169
170 fprintf('Duration of effective treatment (days) \n');
171 fprintf('Median Duration: %d\n',nanmedian(delta_t));
172 fprintf('Mean Duration: %d\n',nanmean(delta_t));
173 fprintf('SD Duration: %d\n',nanstd(delta_t));
174 fprintf('\n');
175
176
177 %  Mutants Statistics
178
179
180 fprintf('Mutant Statistics \n\n');
181
182
183 % Mutants at Time of Detection
184
185 fprintf('Number of mutants at tumor detection: \n');
186 fprintf('Median Mutants: %d\n',nanmedian(detect_m));
187 fprintf('Mean Mutants: %d\n',nanmean(detect_m));
188 fprintf('SD  Mutants: %d\n',nanstd(detect_m));
189 fprintf('\n');
190
191
192 % Mutants at the Onset of Treatment
193
```

```
fprintf('Number of mutants at onset of treatment: \n');
fprintf('Median Mutants: %d\n',nanmedian(treat_m));
fprintf('Mean Mutants: %d\n',nanmean(treat_m));
fprintf('SD  Mutants: %d\n',nanstd(treat_m));
fprintf('\n');


fprintf('Quantiles of Mutants: \n');
fprintf('Detection time \n');
fprintf('Quantiles (10%%, 25%%, 75%%, 90%%): %d %d %d %d\n',quantile(
    detect_m,0.1), quantile(detect_m,0.25), quantile(detect_m,0.75),
    quantile(detect_m,0.9));
fprintf('Treatment \n');
fprintf('Quantiles (10%%, 25%%, 75%%, 90%%): %d %d %d %d\n',quantile(
    treat_m,0.1), quantile(treat_m,0.25), quantile(treat_m,0.75),
    quantile(treat_m,0.9));
```

8.2 Main Code

```

function [S, M, m_det, t_det, m_treat, t_treat, t_final, extinct_flag]
    = DT_treatment_Final(Tmax, n_detect, n_treat, n_fail, S0, bsen,
     dsen, Csen, bsen_treat, M0, mu, bmut, dmut, Cmut,
    bmut_treat)

% Set the length of the S and M array
S = 0:Tmax; M = 0:Tmax;

% Initialize values
S(1) = S0;
M(1) = M0;
s = S0;
m = M0;

m_det=NaN;
t_det=NaN;
count_det=0;

```

```
m_treat=NaN;
t_treat=NaN;
count_treat=0;
treatment_flag=0;

t_final=NaN;

extinct_flag=0;

for t=1:Tmax
    % Population goes extinct
    if s + m == 0
        extinct_flag=1;
        break;
    else
        % Tumor size reaches detection level
        if(s + m >= n_detect)
            count_det=count_det + 1;
        end
        if(count_det==1)
            count_det=count_det + 1;
            m_det=m;
            t_det=t;
        end
        % Treatment begins
        if (s + m >= n_treat)
            treatment_flag=1;
            count_treat=count_treat +1;
        end
        if(count_treat==1)
            count_treat=count_treat +1;
            m_treat=m;
            t_treat=t;
        end
        % Treated population exceeds n_fail
        if ((treatment_flag == 1) && (s+m >= n_fail))
            t_final=t;
```

```
54              break; % end simulation
55          end
56
57          % Determine # of events
58
59          % During treatment
60          if(treatment_flag==1)
61              brate_sen = bsen_treat/(1 + Csen*(s+m));
62              births_sen = mpoiss(s*brate_sen);
63              deaths_sen= mpoiss(s*dsen);
64              brate_mut = bmut_treat/(1 + Cmut*(s+m));
65              births_mut = mpoiss(m*brate_mut);
66              deaths_mut = mpoiss(m*dmut);
67
68          % Before treatment
69          else
70              brate_sen = bsen/(1 + Csen*(s+m));
71              births_sen = mpoiss(s*brate_sen);
72              deaths_sen = mpoiss(s*dsen);
73              mutations = mpoiss(births_sen*mu);
74              brate_mut = bmut/(1 + Cmut*(s+m));
75              births_mut = mpoiss(m*brate_mut);
76              deaths_mut = mpoiss(m*dmut);
77          end
78
79          % Population sizes
80          s = s - deaths_sen + births_sen - mutations;
81          m = m - deaths_mut + births_mut + mutations;
82
83          S(t+1) = s;
84          M(t+1) = m;
85
86      end
87
88
89
90  end
```

```
91
92
93 % Hybrid Poisson random number generator
94
95 function X = mpoiss(mean)
96
97 threshold = 1000; % Threshold value for stochastic or deterministic
98
99 % Stochastic
100 if (mean < threshold)
101     X = poissrnd(mean);          % Simulate a poisson rv
102
103 % Deterministic
104 else
105     X = mean;                % Use the mean (expected number of _ events)
106
107 end
```